OPTICAL PRINCIPLES, BIOMECHANICS, AND INITIAL CLINICAL PERFORMANCE OF A DUAL-OPTIC ACCOMMODATING INTRAOCULAR LENS (AN AMERICAN OPHTHALMOLOGICAL SOCIETY THESIS)

BY Stephen D. McLeod MD

ABSTRACT

Purpose: To design and develop an accommodating intraocular lens (IOL) for endocapsular fixation with extended accommodative range that can be adapted to current standard extracapsular phacoemulsification technique.

Methods: Ray tracing analysis and lens design; finite element modeling of biomechanical properties; cadaver eye implantation; initial clinical evaluation.

Results: Ray tracing analysis indicated that a dual-optic design with a high plus-power front optic coupled to an optically compensatory minus posterior optic produced greater change in conjugation power of the eye compared to that produced by axial movement of a single-optic IOL, and that magnification effects were unlikely to account for improved near vision. Finite element modeling indicated that the two optics can be linked by spring-loaded haptics that allow anterior and posterior axial displacement of the front optic in response to changes in ciliary body tone and capsular tension. A dual-optic single-piece foldable silicone lens was constructed based on these principles. Subsequent initial clinical evaluation in 24 human eyes after phacoemulsification for cataract indicated mean 3.22 diopters of accommodation (range, 1 to 5 D) based on defocus curve measurement. Accommodative amplitude evaluation at 1- and 6-month follow-up in all eyes indicated that the accommodative range was maintained and that the lens was well tolerated.

Conclusions: A dual-optic design increases the accommodative effect of axial optic displacement, with minimal magnification effect. Initial clinical trials suggest that IOLs designed on this principle might provide true pseudophakic accommodation following cataract extraction and lens implantation.

Trans Am Ophthalmol Soc 2006;104:437-452

INTRODUCTION

Accommodation in the youthful phakic eye is achieved by constriction of the ciliary muscle that leads to increase in the central convexity of the crystalline lens.[1-3] Although some details of the anatomy and physiology remain to be elucidated, the most consistent evidence available to date supports the description attributed to Helmholtz, whereby at rest (and at distance focus), the supporting equatorial zonules maintain tension on the crystalline lens, flattening the central curvature of the lens. Ciliary body constriction leads to the release of zonular tension, thus allowing the anterior and posterior surfaces of the lens to bow outward and increasing the converging power of the eye.

An inexorable loss of accommodative amplitudes accompanies maturity, and this presbyopic change has been attributed to various causes that include reduced ciliary body function,[4] changes in the geometric relationships of the lens and the surrounding zonular and ciliary body structures based on progressive circumferential enlargement of the crystalline lens,[5-7] and changes in the elastic properties of the lens substance and capsule.[8,9] Whereas Croft and coworkers[9] have reported an age-dependent decline in amplitude and velocity of ciliary body movement during accommodation driven by midbrain electrical stimulation, the same laboratory has described little age-dependent difference in the contractile response of isolated rhesus monkey ciliary body to muscarinic agonists.[10]

Based on the assumption that some useful ciliary muscle strength persists into senescence, various attempts have been made to replace the sclerotic lens with a pliable material that reproduces both the optical and biomechanical properties of the accommodating crystalline lens.[11-21] In general, two approaches have been taken, one whereby the crystalline material is replaced by a gel-filled balloon,[12-14] and the other whereby the capsular bag is refilled directly with a polymer with elastic properties that approach that of the youthful crystalline lens.[15-21] Early studies reported by Nishi and coworkers[12-14] using the technique of endocapsular balloon inflation in a primate model reported relatively low accommodative effect that decreased over time due to capsular bag fibrosis. Haefliger and Parel[15] have also investigated direct capsule bag refilling in a primate model and reported accommodative change under pilocarpine stimulation. However, critical review has questioned the interpretation of these studies, because the measurement of accommodative effect was based indirectly upon changes in anterior chamber depth that may well be attributed to anterior rotation of the ciliary body and subsequent lens displacement under the influence of pilocarpine, unrelated to accommodative lens shape change.[20]

More recent studies of capsule bag refilling using injectable silicone in primate eyes have used automated refractometry following pilocarpine stimulation.[19] However, in all cases, anterior and posterior capsule opacification precluded measurements at 3 months. Moreover, a relatively generous capsule fill was required to create sufficient tension for an accommodative effect, but this produced highly ametropic eyes with unpredictable refractive error.

Although this approach has great promise, significant technological and biological obstructions persist; the material property demands are such that a deformable gel must have enough rigidity to maintain a specific shape (and thus optical power) over time, while having elastic properties that will allow rapid, predictable, and sustained response to equatorial tension and release as demanded

From the Department of Ophthalmology, University of California San Francisco, San Francisco, California. Dr McLeod has a financial interest in Visiogen Inc and in the device described herein. He owns founding stock in Visiogen Inc and has received research support and travel reimbursement from Visiogen Inc.

by the dynamics of accommodation.[21] Moreover, the baseline optical power of the capsule-filling gel must be predictable so as to produce emmetropia at rest, the interface between gel and capsular bag must be resistant to cellular proliferation following cataract extraction, and the system must be relatively insensitive to the changing elasticity of the capsular bag associated with capsular fibrosis.

An alternative to filling the capsular bag with a flexible gel was described by Hara, [22] who suggested that anterior axial displacement of a plus-power rigid optic would produce a myopic shift replicating the effect of accommodation. He thus proposed filling the capsular bag with a rigid shell rather than a gel, such that the shell was composed of two lenses, 8 mm in diameter, connected by a polypropylene coil spring. The capsular bag would compress the complex, but ciliary body constriction would lead to release in capsular bag tension and separation of the optics. Later, the design was modified such that the pair of rigid polymethylmethacrylate 6-mm diameter optics were connected by four peripheral closed polyvinylidene fluoride flexible haptics separating the optics by 3.0 mm. The anterior lens was assigned the optical power of the system while the posterior plano lens and haptics served to transmit zonular and capsular tension to the complex.[22]

Contemporary intraocular lens (IOL) designs continue to exploit the accommodative effect of anterior lens displacement. The HumanOptics (Erlangen, Germany) and Crystalens (Aliso Viejo, California) accommodative IOLs both employ hinged connections between the optic and supporting haptics that permit anterior displacement of the optic in response to ciliary body constriction. Coleman[23,24] has proposed that vitreous pressure may play a central role in translating ciliary body contraction to lens deformation and accommodative change. In this model, the lens, zonules, and anterior vitreous form a diaphragm separating the anterior and posterior segments, such that during accommodation a pressure differential is generated between these compartments. Accommodative IOLs designed to undergo axial displacement in response to increased ciliary body tone are thought at least in part to be responding to the hydraulic effect of vitreous pressure.[25]

Early clinical evaluation has confirmed some degree of accommodative effect. Recently, Langenbucher and colleagues[26] have reported using multiple measurement methods extensive evaluation of a cohort of patients in whom the HumanOptics 1CU accommodative IOL had been implanted as compared to an age-matched control group in which a single-optic nonaccommodative lens had been implanted. Based on demonstrable changes in anterior chamber depth that followed pilocarpine-induced ciliary body constriction, these researchers were able to confirm some degree of optic displacement consistent with the putative mechanism of accommodative action, but the most generous measure of accommodation range (as measured by best distance corrected near point) was limited to a mean of 1.6 D (range, 0.50 to 2.56 D). This range did, however, exceed that measured for eyes implanted with a monofocal lens, which demonstrated a mean accommodation amplitude of 0.42 D (range, 0 to 0.75D).

A less rigorous treatment of the Crystalens AT-45 accommodative IOL has been reported by Cumming and colleagues.[27] Based exclusively on visual acuity measured at various distances, these investigators have suggested accommodative function producing best distance corrected near acuity of J3 in 96% of patients. However, the peer-reviewed literature to date does not include an evaluation of axial displacement upon which the accommodative function of this system depends. Findl and colleagues have employed optical partial coherence interferometry to evaluate the axial displacement of this lens following pilocarpine ciliary body stimulus but have failed to demonstrate any significant axial movement. (unpublished data, Findl et al, Annual Meeting of the European Society of Cataract and Refractive Surgeons, Munich, Germany, 2003). In general, these studies suggest limited accommodative range consistent with the optical constraints of minimal anterior displacement of a relatively low-power lens.

Heatley and colleagues[25] have modeled the performance of an accommodative lens design based upon the principle of increased vitreous pressure pushing the lens capsule forward as a circular diaphragm. In this model, the lens was treated as a simple piston displaced anteriorly by vitreous pressure and constrained in forward movement by intrinsic lens design and anterior ocular structures. They demonstrated that the displacement achieved is dependent not only upon the pressure exerted on the capsule from the vitreous, but also on the thickness and elasticity of the capsule, the tangential stress exerted on the capsule, and the diameter of the capsular bag. They therefore proposed that inconsistency in the performance of these lenses noted clinically might be explained in part by variable axial displacement due to variability in capsule thickness and capsular bag diameter.

Ray tracing analysis indicates that the degree of accommodative effect is related not only to the degree of displacement of the moving lens, but also to the power of the displaced lens.[28] A simple and rough approximation of the change in conjugation power of the system is provided by the following formula: $\Delta Dc \simeq (Dm/13)\Delta s$ where ΔDc is change in conjugation power of the eye, Dm is the dioptric power of the moving lens, and Δs is the change in lens position expressed in millimeters.[28] Studies examining changes in anterior chamber depth as an indicator of optic displacement suggest that axial movement is typically limited to less than 1 mm.[29,30] This is expected to produce limited and variable accommodative effect for the range of IOL powers (+15 to +25 diopters [D]) most commonly implanted following cataract surgery.

If indeed the degree of accommodative shift produced by forward axial displacement of a plus-power IOL is proportional to the power of the lens, then an accommodative lens can be designed based on the principle of a high plus-power moving lens coupled to a stationary optically compensatory minus lens that would produce more consistent, higher-amplitude accommodative shifts than current systems based on axial lens displacement, while circumventing the biomechanical constraints of flexible gels.[28] Moreover, a system of spring haptics joining the two can be designed to translate changes in ciliary body tone to axial displacement and thus optical power change.[28]

The lens arrangement of a plus-power lens coupled to a minus lens forms a simplified telephoto optical system that is similar to a Galilean telescope configuration, with the important difference that the telephoto system creates the image at a finite and relatively short distance from the lenses (in this case, the retina) while a Galilean telescopic system includes a plus lens coupled to a minus eyepiece located within the prime focus of the plus lens so as to create a near-collimated beam that the eye can then bring to focus

with minimal accommodative effort.[31,32]

The fact that there is a relationship between the telephoto design of a dual-optic accommodative IOL and telescope optics has implications for the potential role that magnification might play in the function the IOL. A primary concern is that magnification leading to significant image size disparity (aniseikonia) may preclude monocular implantation if the other eye remains phakic or is corrected with a single-optic IOL. Moreover, magnification might confound the interpretation of near vision functional testing, because improved performance compared to single-optic designs might be attributed to magnification effect rather than a true change in the conjugation power of the eye.

Therefore, a secondary ray tracing analysis was performed to study the potential effect of magnification on the optical performance of a dual-optic accommodative IOL system.

This design and development process was based on optical ray tracing and biomechanical finite element modeling, prototype fabrication, cadaver eye testing, and subsequent prototype modification culminating in initial clinical trials reported herein.

METHODS

OPTICAL DESIGN

Given that a major limitation to the change in conjugation power induced by anterior lens displacement is the power of the lens, it is necessary to first quantify theoretically the effect of axial displacement of a typical accommodative lens in the human eye and then compare this to the effect of an alternative optical arrangement in which the power of the system is divided into a high plus-power anterior moving optic coupled to a static minus power posterior optic. Ray tracing analysis software (ZEMAX, Focus Software Inc, Tucson, Arizona) using a theoretical model eye was used to analyze the expected optical effect of 1-mm axial movement of a single IOL located at the plane of the posterior capsule.[28] Assumptions used in constructing the model are listed in Table 1.[28]

TABLE 1. CONSTANTS USED IN GENERATING THE THEORETICAL MODEL EYE[28]

Cornea index of refraction	1.3771
Aqueous index of refraction	1.3374
Lens index of refraction	1.42
Vitreous index of refraction	1.336
Cornea aspheric anterior vertex radius	7.8 mm
Cornea aspheric posterior vertex radius	6.5 mm
Cornea thickness	0.55 mm
Anterior chamber depth	3.05 mm
Second nodal point, posterior to corneal apex	7.51 mm
Axial length	23.86 mm

Conjugation power change was calculated as change in refraction at the spectacle plane with vertex distance to the posterior spectacle surface of 12 mm, and modeled over a range of theoretical lens powers from +15 to +30 D. For purposes of comparison, the model was then used to calculate conjugation power change induced by anterior lens axial displacement of 1 mm for a dual-optic system with a 32 D anterior optic and a 0.5-mm posterior compensatory minus lens with power varied to produce a system ranging from +15 to +30 D.[28]

The degree of image magnification produced on the retina by a dual-optic system was compared to that of a single-optic system with the lens 4 mm and 5 mm posterior to the posterior surface of the cornea, for model eyes with three axial lengths: short (22.2 mm), medium (23.25 mm), and long (25.5 mm) (Table 2 and Appendix 1).

As described by Langenbucher and colleagues,[33] any optical system can be considered a combination of refracting surfaces and interspaces between the surfaces. The angles at which a given ray meets and exits a refracting surface (ie, refraction), as well as deviation from the optical axis that occurs during the passage of the ray through the interspace (translation), can be described as a linear coordinate transformation and specified in matrix form.[34,35] The corresponding matrix of the optical system is called power matrix: Equation 1 $S = \begin{pmatrix} a & b \\ c & d \end{pmatrix}$

This power matrix is generated by specifying the refraction and translation matrices of all elements of the optical system and then multiplying them together in reverse order.

$P = \begin{pmatrix} 1 & -R \\ 0 & 1 \end{pmatrix}$, refraction matrix of the surface with refractive power R $T = \begin{pmatrix} 1 & 0 \\ t/n' & 1 \end{pmatrix}$, translation matrix of interspace (t) and medium refractive index (n′) The system power matrix now can be defined as Equation 2 $S = P_k \bullet T_{k-1} \cdots P_2 \bullet T_1 \bullet P_1$

A reduced eye model[36] was utilized in this analysis where the refractive powers of the anterior and posterior corneal surfaces were combined so that corneal power could be defined by a single surface.

This power matrix was applied to both the dual-optic IOL configuration and to the single-optic IOL. Telephoto optical systems manifest the greatest degree of magnification when the optics are most widely separated. Therefore, in order to model the scenario associated with the greatest degree of magnification in a dual-optic IOL, the lenses were set at the maximal separation for which the system is designed, 1.5 mm. This is expected to produce about 4 D of object vergence (250-mm distance between the corneal vergence and object location).

TABLE 2. EYE AND LENS PARAMETERS USED TO MODEL THE RETINAL IMAGE MAGNIFICATION OCCURRING IN SHORT, MEDIUM, AND LONG EYES FOR 4 D OF OBJECT VERGENCE

PARAMETER	VALUE	DEFINITION
Axial Length	22.2	"Short" eye
	23.25	"Medium" eye
	25.5	"Long" eye
R_1	43.25	K-reading
t_1 (ACD)	4	Dual optic
	5	Single optic
r_2	5.963	Anterior lens front surface radius of dual optic
	6.0	Front surface radius of single optic
t_2	1.3	Anterior lens thickness or single optic thickness
r_3	–5.963	Anterior lens back surface radius of dual optic
	–5.4	Back surface radius of single optic (short eye)
	–7.5	Back surface radius of single optic (medium eye)
	–26.6	Back surface radius of single optic (long eye)
t_3	1.5	Anterior to posterior lens separation in dual optic
r_4	–7.25	Posterior lens front surface radius of dual optic
t_4	0.535	Posterior lens thickness in dual optic (short eye)
	0.525	Posterior lens thickness in dual optic (medium eye)
	0.375	Posterior lens thickness in dual optic (long eye)
r_5	–7.81	Posterior lens back surface radius of dual optic (short eye)
	–13.343	Posterior lens back surface radius of dual optic (medium eye)
	–24.082	Posterior lens back surface radius of dual optic (long eye)

ACD = anterior chamber depth.

Table 2 lists the eye model and lens parameters used for the evaluation.

The eye and dual-optic parameters then are converted to the parameters defining the refraction and translating matrices (see Table A of Appendix 2).

The power matrix of the system (Eq 1) then can be constructed according to Eq 2 and the locations of the system cardinal points can be then determined. Table B of Appendix 2 lists the definitions of the cardinal points in power matrix terms as well as the focal length and image-object magnification as their derivatives.

BIOMECHANICAL DESIGN

A review of the literature suggested the following biomechanical constraints within which an accommodating IOL must function. The typical diameter of the crystalline lens is about 9.5 mm, with a thickness of about 4.5 mm. Following extracapsular cataract extraction, the capsular bag is estimated to be 10.5 mm in diameter.[37] The force generated by the ciliary body even in the presbyopic eye is estimated to be 1 gram force (~10 mN).[38]

In order to respond to ciliary body action, energy must be stored and released in the system. A lens complex was designed with optics linked by articulations that, at rest outside the capsular bag, are widely separated. When implanted within the capsular bag, radial bag tension should compress the optics axially, reducing the interoptic separation and thus generating strain energy in the interoptic articulations. With accommodative effort, the zonules relax, releasing the tension on the capsular bag, thus allowing release of the strain energy and anterior displacement of the anterior optic.

In the disaccommodated (far vision) position, the optics should be pulled together by the capsular bag, whereas in the accommodated (near vision) position, the lenses should move apart under the spring force of the haptics. Thus, in the closed, or disaccommodated, distance position: **zonule/capsule tension – ciliary body force > spring force of lens**

However, in the open, accommodated, near position: **zonule/capsule tension – ciliary body force < spring force of lens**

That is to say, in the disaccommodated state (distance focus), the ciliary body force is minimal, and the restoring force of the zonule and capsule structures are great enough to overcome the spring force of the IOL complex, so that the IOL optics are compressed. With accommodation (near focus), the restoring force of the zonule and capsule complex is counteracted or relieved by ciliary body force (assumed to be at its maximum approximately 10 mN), allowing the zonules to move centripetally, thus releasing the IOL complex for anterior-posterior expansion to an accommodated state. The system is therefore in varying states of force balance, but accommodation occurs with the change in displacement of the apparatus under muscle force contraction, reducing the restoring force of the zonules and capsule to the point that the spring force of the haptics can produce anterior lens displacement.

Finite element modeling was applied to design the parameters of the interoptic articulations and optics using a commercially available PC-based software package (COSMOS DesignSTAR, Structural Research and Analysis Corp, Santa Monica, California). The following two material properties were entered into the model: (1) elastic modulus in tension, and (2) Poisson's ratio, for a nearly incompressible, rubber-like material.

The entire lens was modeled with 10-node, solid tetrahedral elements. Element size was automatically varied to accurately represent the stress gradients in areas where stress concentration might occur. The posterior surface of the back lens was rigidly constrained in all directions. A unit displacement load was applied to the anterior surface of the front lens directed along the optic axis toward the back lens. Linear and nonlinear static analyses were performed. The resisting force under the applied load, stresses in the entire lens, and deformation of each node were calculated.

Assuming some degree of elasticity in the peripheral capsular bag, as the anterior optic moves in the anterior and posterior directions, it was assumed that there would be some change in the volume of aqueous captured between the optics within the capsular bag. Therefore, in order to facilitate fluid exchange, protuberances on the anterior optic were incorporated, thus tenting the capsulorrhexis edge up from the front surface of the optic and preserving an avenue for aqueous flow.

INITIAL PROTOTYPE DESIGN AND CADAVER EYE TESTING

Based on the dual-optic spring haptic design generated by the optical and biomechanical models described above, a prototype was generated.[28] An exhaustive review of the literature suggested that the risk of interlenticular opacification was greatly reduced with double optic designs using silicone,[39-46] so this material was used in the fabrication of initial foldable prototypes. As previously reported, a human cadaver eye model was used to examine the ergonomics of folding and implantation, the anatomical relationship between the lens in its endocapsular location and other anterior segment structures, and stability within the capsular bag.[28]

A series of experimental implantations was performed whereby phacoemulsification of the crystalline lens via a clear corneal incision was performed in a cadaver eye with irrigation and aspiration of cortical material.[28] The wound was enlarged to approximately 4.0 mm, and the prototype lens was placed in folding forceps and inserted into the capsular bag. In cases where corneal clouding precluded standard phacoemulsification, a central 8-mm trephination in the central cornea was performed, followed by open sky cataract extraction and lens implantation, after which the corneal button was sutured back into place. Ultrasound biomicroscopy of the eye was then performed to image the location and orientation of the IOL in situ.

INITIAL CLINICAL TRIALS

A limited pilot study to investigate the clinical performance of the dual-optic accommodative device was initiated. All tenets of the Helsinki Declaration for the Protection of Human Subjects in Medical Research were strictly observed, independent institutional review board approval was obtained, and signed informed consent was obtained from all participants.

Surgical Procedure

Patients considered for inclusion were those 40 years or older with visual loss and cataract that required removal, who had the ability to fully comprehend the informed consent and who were considered likely to adhere to the postoperative examination schedule and demands. Exclusion criteria included visual impairment of the fellow eye, corneal astigmatism greater than 2 D, significant anterior segment pathology including glaucoma or potentially occludable angles, capsular exfoliation, ocular inflammation or poor pupillary dilation, and systemic diseases such as autoimmune disease and diabetes.

Preoperative testing included a complete ophthalmic examination as well as measurement of corneal curvature, anterior chamber depth, lens thickness, and axial length. These measures were entered into a theoretical model eye that was modified to describe the appropriate power distribution of the plus and minus components of the dual-optic lens for each individual patient.

Standard phacoemulsification via a clear corneal or scleral wound was performed. A capsulorrhexis ranging in diameter from 4.5 to 5.5 mm was created, and the nucleus and cortical material were removed using an endocapsular technique. Careful polishing of the anterior lens capsule was performed in order to diminish lens epithelial cell proliferation over the anterior capsule and reduce the

incidence of anterior capsule opacification, a theoretically limiting factor for lens performance. The wound was enlarged to 4.5 mm, and using folding forceps, the dual-optic lens was placed through the capsulorrhexis into the capsular bag in a single-step procedure. Extensive aspiration of residual viscoelastic was performed, with particular attention to the space between the posterior optic and the posterior capsule, and the gap between the two optics. At the end of the procedure, the wound was secured using interrupted 10-0 nylon sutures. Postoperative medications included atropine 1%, one drop at the end of the procedure and one drop on the first postoperative day, topical corticosteroids (prednisolone acetate 1%) for 6 weeks, and antibiotics (ofloxacin 0.3%) for 1 week.

Postoperative Examinations

Postoperative examinations were designed in order to evaluate both potential complications and adverse events as well as the performance of the dual-optic design.

Complications. Postoperative examination included measurement of uncorrected and best-corrected distance vision using a LogMAR EDTRS chart at 4m with luminance standardized to 85 cd/m^2 using the Vector Vision CVS 1000 light box, intraocular pressure, and pachymetry, as well as an assessment of corneal clarity, anterior segment inflammation, prelenticular or interlenticular opacification, angle occlusion, lens centration and orientation, iris anatomy, and posterior segment status.

Performance. Postoperative examination included measurement of residual refractive error and uncorrected and best distance-corrected near visual acuity using a Rosenbaum near card held at 40 cm.

Defocus curves were generated in order to characterize near function. The untested eye was occluded, and the best distance correction was placed in the phoropter or trial lens set. Plus lenses were added in 0.50 D steps, and the visual acuity was recorded at each step. Defocus was continued until the baseline best-corrected vision had fallen by at least 3 lines. Returning to the best distance correction, the procedure was repeated with the addition of minus lenses in 0.50 D steps. Defocus was continued until vision had fallen by at least 3 lines. Accommodative range was defined by the range of lens powers beyond which distance visual acuity was reduced by 2 lines on the EDTRS chart.

To provide a measure of comparison, a cohort of 10 patients who had undergone uncomplicated cataract extraction at least 6 months earlier with implantation of a single-optic standard acrylic (Acrysof MA60AC, Alcon Corp, Fort Worth, Texas) or silicone (Allergan Inc, Irvine, California) IOL and who had best-corrected visual acuity of 20/20 or better were similarly tested and defocus curves generated.

To obtain objective data demonstrating the mechanism of action of the dual-optic accommodative IOL design, high-resolution ultrasound biomicroscopy was performed using a 35-MHz ultrasound probe (Ophthalmic Technologies Inc, Canada) on a small number of selected patients. Patients were selected for this study based on their ability to cooperate with the examination procedure and on their willingness to be subjected to this additional, somewhat demanding testing. In order to stimulate accommodation, with the subject in a recumbent position and the ultrasound immersion probe placed over the study eye, a near reading target was held in front of the contralateral eye and the subject was instructed to make his or her best attempt to read. Based on the difficulty posed by presenting a reading target to a recumbent patient with the cumbersome immersion ultrasound positioned over the study eye, and the presbyopic status of the fixing eye that compromised reading ability, the author elected to also study lens movement driven by a pharmacologic accommodative stimulus. Six percent pilocarpine was applied to the study eye to stimulate accommodation, and the position of the anterior and posterior optic surfaces relative to the corneal plane were imaged.

If pharmacologic accommodative stimulation was used, on a separate day, 1% cyclopentolate was administered to the eye, and the imaging was repeated to assess the position of the anterior and posterior optic surfaces in the disaccommodated state. If a near target was used to stimulate accommodation, this test was performed on the same day. The images generated were then evaluated to describe the separation of the anterior and posterior optics under accommodated and disaccommodated conditions, as well as the distance from the posterior corneal plane to the anterior surfaces of the anterior and posterior optics, as a measure of lens separation vs displacement of the entire complex.

RESULTS

OPTICAL DESIGN

As reported previously, ray tracing analysis of various scenarios modeled consistently demonstrated that anterior displacement of an exaggerated plus-power optic coupled to a compensatory static minus lens produced greater change in object distance compared to identical displacement of a single-optic lens of similar composite power.[28] Figure 1 demonstrates the degree of accommodative change for 1-mm displacement of a dual-optic system with a 32 D anterior optic separated by 0.5 mm from the appropriately powered posterior minus lens in the resting state as compared to 1-mm displacement of a single-optic lens. As expected, the optical efficiency of the single-optic system rises to meet that of the dual-optic system as the power of the optic is increased.

The positions of the cardinal points and their derivatives, including image-object magnification, are presented for the dual-optic IOL (Table 3), and for the single-optic IOL (Table 4). The values of the cardinal points are provided in terms of eye anatomical characteristics, ie, distance from the corneal vertex. Negative values refer to the location to the left from the vertex, and positive to the right from the vertex.

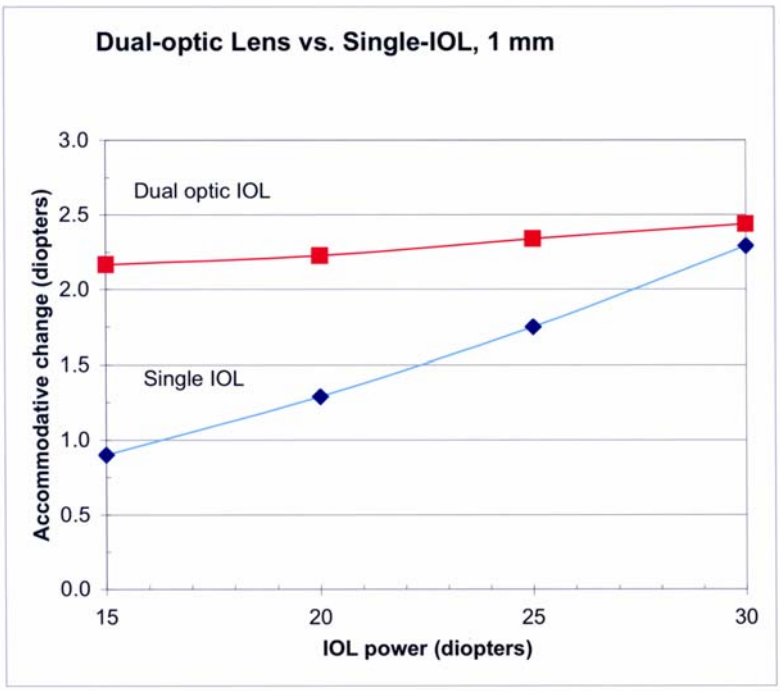

FIGURE 1

Accommodative change calculated by ray tracing analysis for 1-mm movement of a single-optic intraocular lens (IOL) for powers ranging from 15 to 30 diopters compared to a dual-optic IOL with a 32 diopter anterior moving lens coupled to a variably powered static posterior lens. Constants used in the model eye are listed in Table 1. The curves demonstrate that at high lens powers, the accommodative effect of axial displacement of a single lens is similar to that of the dual-optic design, but while the accommodative effect is preserved at low powers in a dual-optic system, that effect is greatly reduced at low powers for a single-optic lens.

TABLE 3. RETINAL IMAGE MAGNIFICATION CALCULATED IN SHORT, MEDIUM, AND LONG EYES WITH 4 DIOPTERS OF VERGENCE FOR A DUAL-OPTIC INTRAOCULAR LENS: CARDINAL POINTS AND THEIR DERIVATIVES

PARAMETERS	SHORT EYE	MEDIUM EYE	LONG EYE
Dual-optic eye system power matrix	$\begin{pmatrix} 0.8888 & -69.636 \\ 0.0052 & 0.71669 \end{pmatrix}$	$\begin{pmatrix} 0.9185 & -65.568 \\ 0.0052 & 0.71711 \end{pmatrix}$	$\begin{pmatrix} 0.9697 & -58.129 \\ 0.0051 & 0.72465 \end{pmatrix}$
First focal point (F_1)	-12.76	-14.008	-16.682
Second focal point (F_2)	21.085	21.937	23.83
First principal point (P_1)	1.597	1.244	0.521
Second principal point (P'_2)	1.900	1.561	0.847
First nodal point (N_1)	6.422	6.368	6.301
Second nodal point (N'_2)	6.725	6.685	6.627
First focal length (EFL_1)	14.36	15.25	17.203
Second focal length (EFL_2)	19.185	20.376	22.984
Image distance from second principal point	20.30	21.69	24.65
Image vergence in diopters	65.811	61.60	54.19
Object distance from first principal point	-261.47	-251.87	-253.97
Image vergence in diopters	3.824	3.97	3.94
Magnification ($M_{dual\text{-}optic}$)	-0.05811	-0.06445	-0.07266

The optical effect of the telephoto type construction of the dual-optic IOL is that of shifting the cardinal point toward the object from the locations of the equivalent cardinal points of a single-optic IOL for the same eye configuration. This results in a slight

increase in focal lengths and magnification.

One can express the relative increase in magnification by application of the following formula $\Delta M = \frac{M_{dual-optic} - M_{\sin gle-optic}}{M_{\sin gle-optic}}$

This leads to the calculation of a relative increase in magnification by 1% for the "short" eye, 2.16% for the "medium" eye, and up to 2.5% for the "long" eye.

TABLE 4. RETINAL IMAGE MAGNIFICATION CALCULATED IN SHORT, MEDIUM, AND LONG EYES WITH 4 DIOPTERS OF VERGENCE FOR A SINGLE-OPTIC INTRAOCULAR LENS: CARDINAL POINTS AND THEIR DERIVATIVES

PARAMETERS	SHORT EYE	MEDIUM EYE	LONG EYE
Single-optic eye system power matrix	$\begin{pmatrix} 0.857 & -70.9297 \\ 0.0046 & 0.78661 \end{pmatrix}$	$\begin{pmatrix} 0.8801 & -66.973 \\ 0.0046 & 0.78661 \end{pmatrix}$	$\begin{pmatrix} 0.9227 & -59.668 \\ 0.0046 & 0.78661 \end{pmatrix}$
First focal point (F_1)	-12.082	-13.14	-15.465
Second focal point (F_2)	21.116	21.99	23.913
First principal point (P_1)	2.017	1.791	1.295
Second principal point (P'_2)	2.281	2.043	1.522
First nodal point (N_1)	6.754	6.808	6.926
Second nodal point (N'_2)	7.018	7.06	7.153
First focal length (EFL1)	14.098	14.93	16.76
Second focal length (EFL_2)	18.836	19.95	22.39
Image distance from second principal point	19.92	21.21	23.98
Image vergence in diopters	67.07	63.00	55.72
Object distance from first principal point	-259.12	-251.59	-253.14
Image vergence in diopters	3.86	3.97	3.95
Magnification ($M_{single-optic}$)	-0.05754	-0.06309	-0.0709

BIOMECHANICAL DESIGN

Based on the parameters entered into the finite element model as described in the "Methods" section, a dual-optic single-piece lens connected by four spring haptics was designed (Figure 2).

The response of the lens to applied loads was varied across numerous prototypes by altering the thickness, length, and angles of the haptics in relation to the optic. The design entered into subsequent studies was constructed using silicone of refractive index 1.43 with length 9.5 mm and width 9.8 mm. When compressed, the total lens thickness was 2.2 mm, and the haptics were designed to allow 1.5 mm of optic movement with relaxation of the capsular bag due to ciliary body contraction.

CADAVER EYE TESTING

As previously reported, multiple cadaver eye implantations of lens prototypes were performed.[28] Under closed conditions, the anterior and posterior optics were compressed, and the lens was folded using standard folding forceps. The lens was inserted with minimal resistance through corneal wounds of internal diameter approximately 4 to 4.5 mm as measured by calipers. Under both open sky and closed conditions, the prototypes could be consistently inserted without difficulty into the capsular bag via an approximately 5-mm capsular opening. Gross examination revealed in all cases a centered lens, and ultrasound biomicroscopy of the lens in situ revealed the anterior optic to be located posterior to the iris without contact between the peripheral iris and the lens complex.

INITIAL CLINICAL TRIALS

Twenty-six eyes of 21 patients were enrolled in the trial reported herein. One patient died of complications of systemic tuberculosis. In another patient, a capsulorrhexis that was considered too large led to lens decentration that required lens explantation. Twenty-four eyes (n = 24) were available for the 6-month follow-up evaluation.

The 21 patients enrolled in the study consisted of eight men and 13 women with an average age of 64.5 years (range, 40 to 78). Preoperative best spectacle-corrected visual acuity ranged from light perception to 20/60. Surgery was uncomplicated with the exception of one case, as indicated above, where a large and slightly decentered capsulorrhexis led to lens decentration requiring explantation. No cases of posterior capsule opacification requiring Nd:YAG laser capsule lysis or interlenticular opacification were observed.

The mean uncorrected visual acuity improved from LogMAR 0.44 (SD, 0.34) at 1 month to LogMAR 0.23 (SD, 0.18) at 6 months (n = 24). This was attributed to a reduction in surgically induced astigmatism resulting from the relatively large sutured cataract

wound. Best-corrected visual acuity (BCVA) improved from LogMAR 0.11 (SD 0.13) to LogMAR 0.04 (SD 0.06). No patient lost lines of vision, and 100% achieved LogMAR 0.18 (20/30) or better BCVA.

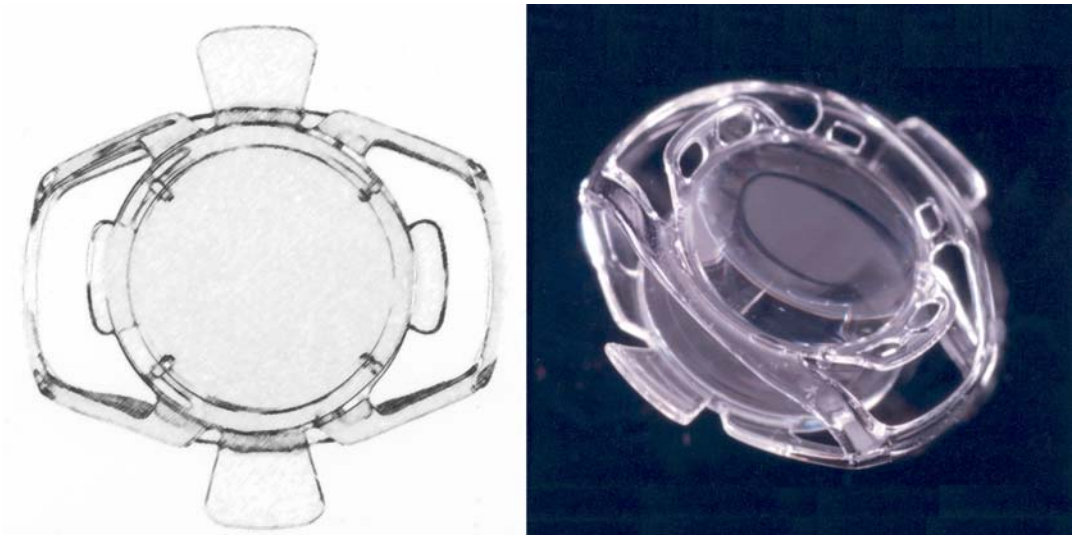

FIGURE 2

Prototype dual-optic accommodative intraocular lens (IOL). Left, Schematic of the anterior surface of the dual-optic accommodative IOL prototype fabricated and tested. The spring haptics are located at the 3- and 9-o'clock positions and stabilizing elements at the 12- and 6-o'clock positions. The entire complex measures 9.8 mm horizontally and 9.5 mm vertically. Right, Photograph of the dual-optic accommodative IOL prototype as viewed in three-quarter profile, demonstrating the high plus-power moving anterior optic (above) coupled to the compensatory minus power static posterior optic (below) by spring haptics. The structures elevated above the plane of the anterior optic are designed to tent the anterior capsule up from the anterior surface of the front optic, allowing aqueous exchange between the interlenticular space and the anterior chamber.

Mean uncorrected near visual acuity values improved from LogMAR 0.11 (SD, 0.18) at the 1-month follow-up to 0.08 (SD, 0.12) at the 6-month visit (n = 24). Distance corrected near visual acuity remained stable, with range of functional vision throughout the course of the study, from 0.17 at 1 month (SD, 0.15) to 0.14 at 6 months (SD, 0.15).

Defocus curves generated for both the dual-optic IOL (n = 24) and for monofocal single-optic lenses (n = 10) are shown in Figure 3. These curves demonstrated that eyes implanted with the dual-optic IOL demonstrated a reduced rate of visual acuity loss (mean accommodative range, 3.22 D; SD, 0.88; range, 1 to 5 D) with defocus compared to eyes implanted with standard, monofocal IOLs (mean accommodative range, 1.65 D; SD, 0.58; range, 1 to 2.5 D; $P<.05$).

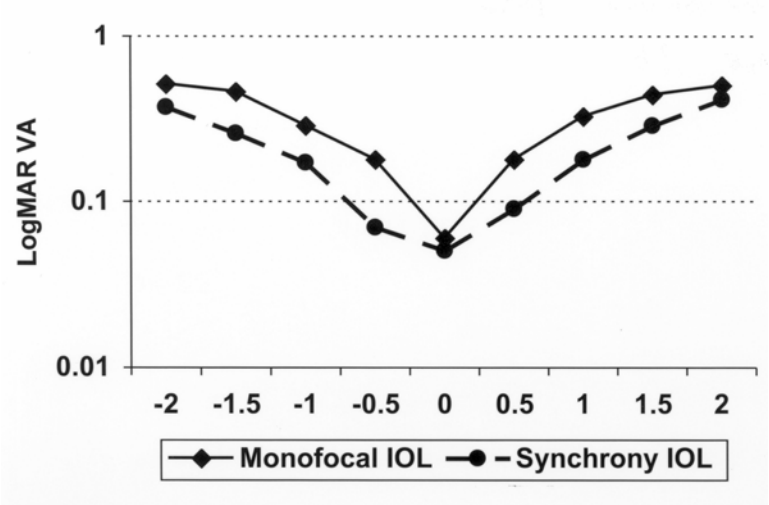

FIGURE 3

Defocus curves generated in 10 eyes with a single-optic (monofocal) intraocular lens compared to 24 eyes with the dual-optic (Synchrony) accommodative lens. The x-axis indicates the power in diopters of the defocusing lens placed in front of the tested eye through which the visual acuity (y-axis) was measured. The accommodative amplitude was defined by the range of defocus lens power through which visual acuity was maintained to within 2 lines on the EDTRS chart.

High-resolution ultrasound biomicroscopy was performed on selected, cooperative patients, in order to evaluate anterior optic displacement with accommodative effort as indicated by increased spacing between the anterior and posterior optics. It was found

challenging to obtain consistent images free of artifact with adequate resolution for interpretation. However, a limited series of interpretable images indicated, under both near target and pharmacologic stimulation, anterior displacement of the anterior optic with increase in the interlenticular separation and minimal posterior optic movement (Figure 4). Because of calibration and orientation inaccuracies, the absolute displacement in millimeters could not be consistently ascertained with confidence.

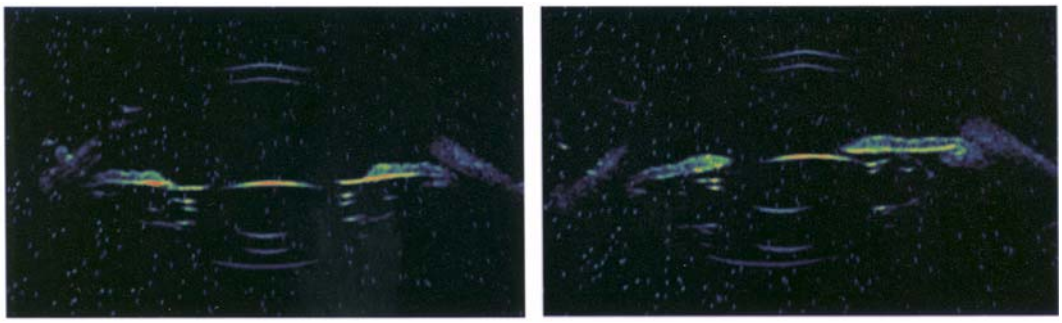

FIGURE 4

High-resolution immersion ultrasound biomicroscopy of the dual-optic intraocular lens in situ. The left panel demonstrates the image obtained in the disaccommodated state after instillation of 1% cyclopentolate. Note the flattened profile of the iris diaphragm, the relatively posterior position of the front optic, and the reduced gap between the anterior and posterior optics. The right panel demonstrates the same eye in accommodation as stimulated by a near target presented to the contralateral eye. Note the anterior vaulting of the iris diaphragm and the reduced anterior chamber depth, as well as the increased separation between the anterior and posterior optics.

DISCUSSION

The optical design presented herein, consisting of a dual-optic system with an exaggerated plus-power optic coupled to a compensatory minus power static lens, can be demonstrated by ray tracing analysis to potentially produce consistent and amplified accommodative amplitude designs across a wide range of implant powers as compared to a single moving optic. This arrangement might be erroneously interpreted as similar to that of a telescopic design, but the spatial arrangement and relative lens powers produce minimal image magnification compared to focal shift. As such, this design is expected to greatly improve the predictability and range of accommodative lens implants and can be considered for monocular as well as binocular implantation.

Whereas in this study commercially available ray tracing software was employed to model the optical effect of a dual-optic accommodative system, Langenbucher and colleagues have used linear geometric matrix analysis based on the Gullstrand eye model to describe the properties of such a system.[33] This alternative analysis confirmed a nearly constant accommodation amplitude in the range of 2.4 to 2.5 D per millimeter. Moreover, these investigators explored the effect of symmetric anterior and posterior translation of the anterior and posterior lenses, respectively, and determined that although this would reduce the accommodative effect compared to anterior movement of the anterior optic with a stationary posterior optic, the focus shift would still exceed that of comparable anterior displacement of a single-optic lens within a similarly modeled eye.

Minimal magnification effect was observed in this analysis of a dual-optic accommodative IOL system. There are two effects to consider where magnification may be clinically significant: (1) the introduction of aniseikonia between the eyes if aphakia in one eye is corrected with a single-optic IOL and in the other with dual-optic IOL; (2) the effect on the visual acuity when evaluating accommodating ability of the dual-optic IOL. The normal tolerance for aniseikonia has been measured as between 5% and 8% by different methods,[47] and image size disparity above this level is expected to prevent fusion leading to a bothersome binocular image and symptoms of aniseikonia.[47-50] The results of this study demonstrate that the upper range of magnification disparity between an eye with single-optic IOL and another with the dual-optic IOL design studied is in the order of 2.5%. This is well below the level at which symptoms due to aniseikonia would be expected to occur, is comparable to the image size disparity established between aphakic contact lens and single-optic IOL correction, and is not expected to impact binocular visual function.

This analysis also allows consideration of the question of whether simply magnification introduced by the dual-optic design rather than a true accommodative change in focal length might lead to improved near vision test results compared to a single-optic lens. To measurably enhance visual acuity based on magnification, the increase in image size should approach the height difference from one test line to the next. In the case of the EDTRS chart, consecutive lines increase in height by a factor of 1.2589.[51,52] Therefore, one might estimate that a magnification increase of 25% would be required to improve testing scores by 1 line. However, the upper range of magnification associated with the dual-optic design seen in this analysis was in the order of 2.5%. This degree of magnification is unlikely to contribute significantly to the performance of the lens.

The spring haptic design allows maximal articulation between capsular tension and the lens system, thus allowing more direct communication with ciliary body tone, since the system is designed to, in effect, fill the capsular bag and expand against both the anterior and posterior capsules. As indicated by this initial clinical study with eyes followed up to 6 months, the compressive effect

against the contracting capsular bag likely contributes to the minimal posterior capsular opacification observed.

The potential effect of increasing capsular rigidity deserves further consideration. The initial clinical data reported herein indicate that accommodative function as suggested by best distance corrected near vision remained stable between 1 and 6 months after surgery, presumably in spite of some degree of capsular contraction and fibrosis. This is consistent with the concept that, in fact, some degree of capsular contraction and rigidity is expected to enhance the mechanical function of the system. In the resting state, in order for zonular tension to be transmitted to the lens complex, the capsular bag must compress the system. This requires some degree of capsular contraction around the lens complex. Subsequent accommodative motion of the lens requires that ciliary body contraction and relaxation be transmitted via changes in zonular and capsular bag tension directly to the lens. Excessive capsule elasticity is expected to attenuate ciliary body and zonular movement; the effect is comparable to that of pulling an object with an elastic band rather than a rope. Progressive capsular fibrosis and contraction will ultimately lead to system failure if the spring force of the system is overwhelmed.

To model the characteristics of capsular fibrosis and opacification as compared to standard, single-optic IOLs, during early development, Werner and colleagues[53] were given access to an early prototype that was implanted in a series of rabbit eyes for study. Prototype lenses designed for the dimensions of the human eye were provided and were not reduced in scale for optimal endocapsular implantation in the rabbit eye. In brief, after bilateral lens extraction was performed in 10 New Zealand white rabbits, the test dual-optic IOL was placed in one eye and a single-piece plate silicone IOL with large fixation holes was placed in the fellow eye that served as a control. Eyes were observed by slit-lamp evaluation up to 3 weeks and graded for ocular inflammatory response, lens fixation and orientation, and anterior and posterior capsule opacification. Animals were sacrificed at 5 to 6 weeks, and the eyes were submitted for gross examination and photography using the posterior Miyake-Apple view, followed by processing for standard light microscopy and staining using hematoxylin-eosin, periodic acid–Schiff, and Masson's trichrome.[53]

In three of 10 eyes, there was partial or complete dislocation of the dual-optic lens forward out of the capsular bag, which was attributed to the relatively large proportions of the prototype that was not scaled down to the dimensions of a rabbit eye. Of the seven study eyes with successful endocapsular retention of the IOL, minimal anterior capsule opacification was observed at all time points as graded subjectively by visual examination of photographs obtained by retroillumination of dilated eyes in vivo and also by visual examination of photographs obtained after enucleation using the Miyake-Apple view, whereas significant fibrosis, opacification, and contraction of the anterior capsule and capsulorrhexis edge were observed in fellow control eyes with the single-optic plate haptic lens. Posterior capsule opacification as assessed by Miyake-Apple view photographs of enucleated eyes graded on a scale of 0 to 4 indicated a significantly higher degree of opacification in the control eyes with the single-optic plate haptic lens as compared to study eyes with the dual-optic accommodative lens (3.14 ± 0.90 compared to 0.71 ± 0.76; $P < .05$).[53]

Although this study provides encouraging data to suggest that the outward pressure exerted on the capsular bag by this expanding lens might be associated with substantial retardation of capsular fibrosis, longer-term studies are necessary to confirm that the retardation of capsular fibrosis noted in the rabbit model extends to the clinical situation and that the minimal capsular opacification noted at 6 months in the initial clinical trial persists.

In this pilot study, the author attempted to investigate both subjective and objective measures of accommodative function. Whereas subjective methods that typically measure visual acuity in the setting of a presumed accommodative stress might reasonably be expected to be indicative of an individual's near vision function, none will reliably distinguish between pseudoaccommodation (for example, due to multifocality) and a true change in the conjugation power of the eye. Retinoscopic methods that include skiascopy, infrared optometry, and wavefront analysis can in theory provide an objective method of measuring accommodative change, but all have proven far more challenging in the research setting than is immediately obvious.[54] The measuring device or experimental set-up frequently interferes with or requires alteration of typical accommodative cues, leading to significantly reduced measured accommodative amplitudes even in cooperative subjects. Moreover, the convergence that accompanies accommodation can present alignment difficulties during measurement as the target is moved. Although this effect can be circumvented by pharmacologic stimulation of accommodation, recent evidence suggests that this technique does not accurately represent physiologic accommodation.[55]

Devices and techniques based on retinoscopy require adequate imaging from the retina that can usually be obtained in the case of young, phakic subjects, but is frequently compromised in older myopic patients where the entrance pupil is often miotic and cataractous change or reflections from implant surfaces distort the image. This report does not include a description of the farrago of devices and techniques to which individuals within the initial cohort were subjected, because virtually all proved irreproducible, unreliable, and impractical in the setting of older, pseudophakic subjects. However, ongoing studies include communication with a number of device developers and manufacturers with the goal of addressing the unique technical challenges that have been encountered.

Based on multiple modes of evaluation, subjective and objective data are presented that suggest both proof of principle and indicators of clinical function of the dual-optic accommodative lens. Best distance corrected near vision better than 0.3 LogMAR (20/40 or J3) for 95% of patients is consistent with some degree of accommodative function, as is the comparison of defocus curves generated from eyes implanted with the dual optic as opposed to monofocal lenses. The definition of accommodative range applied to the defocus curve interpretation (visual acuity maintained within 2 lines on the EDTRS chart) is necessarily arbitrary, but direct qualitative comparison of the defocus curves as demonstrated in Figure 3 indicates that better visual acuity is maintained through defocus with the dual-optic lens as compared to monofocal lenses.

It is of critical importance to recognize that subjective tests of near vision do not directly test dynamic accommodative change in

the conjugation power of the eye. It is certainly possible that the dual-optic design might in some way introduce either a multifocal effect or enhanced depth of focus that might account for these findings. The data generated from high-resolution ultrasound biomicroscopy, however, does provide evidence that pharmacologic and near target stimulation and relaxation of the ciliary body lead to the intended anterior and posterior movement of the anterior optic consistent with accommodative function.

Given the technical limitations in evaluating accommodative function and the absence of a single defining test, researchers have been inclined to perform a battery of tests in order to describe the accommodative characteristics of a particular device, including uncorrected and best distance-corrected near vision, defocus curve analysis, skiascopy, automated refraction, wavefront analysis, and in situ imaging of lens movement.[26,54] However, these techniques do not provide an indication of the performance of these devices that would likely incorporate the effect of characteristics such as accommodative acceleration and deceleration, sustain, and optical quality.

Supplemental tests, such as quality-of-life questionnaires and reading speed, have been suggested, but validated protocols that have been demonstrably relevant to accommodative function have not been established for many such tests. With regard to quality-of-life questionnaires, the most relevant tool available is the National Eye Institute's Refractive Error Quality of Life (RQL) instrument that has been specifically designed to assess the subjective visual and functional effects of refractive error and its correction with contact lenses, spectacles, or surgery.[56,57] It has been shown to be an accurate and sensitive instrument in providing information regarding patient status that is not reflected in traditional clinical ophthalmic measures and has been used to study the effects of presbyopia and monovision correction on vision-targeted health-related quality of life.[58] Instruments such as this might prove useful in further evaluating the effectiveness of accommodative devices. Conversely, although reading speed may appear to be a relevant and useful measure, these tests have not been validated as a useful measure of patient satisfaction and daily function with regard to the wide range of tasks that require accommodation and, moreover, are subject to the vicissitudes of the subject's cognitive function, effort, and level of literacy. More sophisticated evaluation of accommodative lens performance will require the development and application of validated, relevant, and reliable subjective tests.

Nevertheless, while recognizing the current limitations of accommodation measurement technique, the author is encouraged by these initial results. The data reported herein appear to support the proposal that a dual-optic system can be designed that will produce an accommodative change in the conjugation power of the eye through anterior and posterior displacement of the anterior optic. No significant magnification was found for either a single or dual lens system at any theoretical eye axial length studied, and magnification effects are therefore unlikely to contribute to the performance of this configuration of a dual-optic design. The pilot study reported represents only a small cohort of patients with limited follow-up, and larger long-term studies are required to reveal the long-term stability, evolution, and characteristics of the accommodative function suggested. Future studies will seek to incorporate objective measurement techniques under development as well as functional tests and quality-of-life assessment.

ACKNOWLEDGMENTS

The author would like to acknowledge the contributions of the following individuals to this research project: Luis G. Vargas, MD, Visiogen Inc, Irvine, California. Dr Vargas contributed to the examination of study patients involved in the clinical trial. Iván L. Ossma, MD, Fundación Oftalmologica de Santander, Bucaramanga, Colombia. Dr Ossma performed cataract extraction and implantation of the prototype dual-optic accommodating IOL and contributed to the data collection from this patient cohort and the analysis of the clinical data. Michelle Trager, MD, University of California San Francisco School of Medicine. Dr Trager participated in the clinical evaluation of accommodative amplitudes in study patients. Val Portney, PhD, Private Consultant, Tustin California. Dr Portney assisted in lens design and ray tracing analysis. Albert Ting, PhD, Visiogen Inc, Irvine, California. Dr Ting assisted in lens design and biomechanical analysis. Drs McLeod, Vargas, Portney, and Ting have a financial interest in Visiogen Inc, and in the device described herein.

REFERENCES

1. Helmholtz H. *Treatise on Physiological Optics*. Translated from the 3rd German ed. Southall JPC, ed. New York: Dover Publications; 1962.
2. Fincham EF. The mechanism of accommodation. *Br J Ophthalmol Suppl* 1937;8:5-80.
3. Glasser A, Kaufman PL. The mechanism of accommodation in primates. *Ophthalmology* 1999;106:863-872.
4. Duane A. Are the current theories of accommodation correct? *Am J Ophthalmol* 1925;8:196-202.
5. Koretz JF, Handelman GH. Modeling age-related accommodative loss in the human eye. *Mathematical Modeling* 1986;7:1003-1014.
6. Schachar RA. Zonular function: a new model with clinical implications. *Ann Ophthalmol* 1994;26:36-38.
7. Gilmartin B. The aetiology of presbyopia: a summary of the role of lenticular and extralenticular structures. *Ophthalmic Physiol Opt* 1995;15:431-437.
8. Tamm E, Lütjen-Drecoll E, Jungkunz E, Rohen JW. Posterior attachment of ciliary muscle in young, accommodating old, and presbyopic monkeys. *Invest Ophthalmol Visual Sci* 1991;32:1678-1692.
9. Croft MA, Kaufman PL, Crawford KS, et al. Accommodation dynamics in aging rhesus monkeys. *Am J Physiol* 1998;275 (Regulatory Integrative Comp Physiol 44):R1885-R1897.
10. Poyer JF, Kaufman PL, Flügel C. Age does not affect contractile responses of the isolated rhesus monkey ciliary muscle to muscarinic agonists. *Curr Eye Res* 1993;12:413-422.

11. Kessler J. Experiments in refilling the lens. *Arch Ophthalmol* 1964;71:412-417.
12. Nishi O, Hara T, Hara T, et al. Further development of experimental techniques for refilling the lens of animal eyes with a balloon. *J Cataract Refract Surg* 1989;15:584-588.
13. Nishi O, Hara T, Hara T, et al. Refilling the lens with a inflatable endocapsular balloon: surgical procedure in animal eyes. *Graefes Arch Clin Exp Ophthalmol* 1992;230:47-55.
14. Nishi O, Nakai Y, Yamada Y, et al. Amplitudes of accommodation of primate lenses refilled with two types of inflatable endocapsular balloons. *Arch Ophthalmol* 1993;111:1677-1684.
15. Haefliger E, Parel JM. Accommodation of an endocapsular silicone lens (Phaco-Ersatz) in the aging rhesus monkey. *J Refract Corneal Surg* 1994;10:550-555.
16. Hettlich HJ, Lucke K, Asiyo-Vogel MN, et al. Lens refilling and endocapsular polymerization of an injectable intraocular lens: in vitro and in vivo study of potential risks and benefits. *J Cataract Refract Surg* 1994;20:115-123.
17. Nishi O, Nishi K, Mano C, et al. Controlling the capsular shape in refilling. *Arch Ophthalmol* 1997;115:507-510.
18. Nishi O, Nishi K, Mano C, et al. Lens refilling with injectable silicone in rabbit eyes. *J Cataract Refract Surg* 1998;24:975-982.
19. Nishi O, Nishi K. Accommodation amplitude after lens refilling with injectable silicone by sealing the capsule with a plug in primates. *Arch Ophthalmol* 1998;116:1358-1361.
20. Koopmans SA, Terwee T, Barkhof J, et al. Polymer refilling of presbyopic human lenses in vitro restores the ability to undergo accommodative changes. *Invest Ophthalmol Vis Sci* 2003;44:250-257.
21. de Groot JH, Spaans CJ, van Calck RV, et al. Hydrogels for an accommodating intraocular lens. An explorative study. *Biomacromolecules* 2003;4:608-616.
22. Hara T, Hara T, Yasuda A, et al. Accommodative intraocular lens with spring action part 1. Design and placement in an excised animal eye. *Ophthalmic Surg* 1990;21:128-133.
23. Coleman DJ. On the hydraulic suspension theory of accommodation. *Trans Am Ophthalmol Soc* 1986;84:846-868.
24. Coleman DJ, Fish SK. Presbyopia, accommodation and the mature catenary. *Ophthalmology* 2001;108:1544-1551.
25. Heatley CJ, Spalton DJ, Boyce JF, Marshall J. A mathematical model of factors that influence the performance of accommodative intraocular lenses. *Ophthal Physiol Opt* 2004;24:111-118.
26. Langenbucher A, Seitz B, Huber S, et al. Theoretical and measured pseudophakic accommodation after implantation of a new accommodative posterior chamber intraocular lens. *Arch Ophthalmol* 2003;121:1722-1727.
27. Cumming JS, Slade SG, Chayet A, and the AT-45 Study Group. Clinical evaluation of the model AT-45 silicone accommodating intraocular lens. *Ophthalmology* 2001;108:2005-2010.
28. McLeod SD, Portney V, Ting A. A dual optic accommodating foldable intraocular lens. *Br J Ophthalmol* 2003;87:1083-1085.
29. Hardman Lea SJ, Rubinstein MP, Snead MP, et al. Pseudophakic accommodation? A study of the stability of capsular bag supported, one piece, rigid tripod, or soft flexible implants. *Br J Ophthalmol* 1990;74:22-25.
30. Lesiewska-Junk, Kaluzny J. Intraocular lens movement and accommodation in eyes of young patients. *J Cataract Refract Surg* 2000;26:562-565.
31. Kingslake R. *Lens Design Fundamentals*. New York: Academic Press;1978:259-268.
32. Smith WJ. Basic optical devices. In: Fischer RE, Smith WJ, series eds. *Modern Optical Engineering: the Design and Optical Systems*. 2nd ed. New York: McGraw-Hill;1990:235-239.
33. Langenbucher A, Reese S, Jakob C, Seitz B. Pseudophakic accommodation with translation lenses—dual optic vs mono optic. *Ophthalmic Physiol Opt* 2004;24:450-457.
34. Rosenblum WM, Christensen JL. Optical matrix method: optometric application. *Am J Optom Physiol Optics* 1974;51:961-968.
35. Keating MP. Lens effectivity in terms of dioptric power matrices. *Am J Optom Physiol Opt* 1981;58:1154-1160.
36. Atchison DA, Smith G. *Optics of the Human Eye*. Philadelphia: Butterworth Heinemann, Elsevier Science; 2003:250-254.
37. Assia E, Apple DJ. Side view analysis of the lens. I. Crystalline lens and the evacuated bag. *Arch Ophthalmol* 1992;110:89-93.
38. Fisher RF. The force of contraction of the human ciliary muscle during accommodation. *J Physiol* 1977;270:51-74.
39. Gayton JL, Apple DJ, Peng O, et al. Interlenticular opacification: clinicopathological correlation of a complication of posterior chamber piggyback intraocular lenses. *J Cataract Refract Surg* 2000;26:330-336.
40. Werner L, Shugar JK, Apple DJ, et al. Opacification of piggyback IOLs associated with an amorphous material attached to interlenticular surfaces. *J Cataract Refract Surg* 2000;26:1612-1619.
41. Eleftheriadis H, Marcantonio J, Duncan G, et al. Interlenticular opacification in piggyback AcrySof intraocular lenses: explantation technique and laboratory investigations. *Br J Ophthalmol* 2001;85:830-836.
42. Trivedi RH, Izak AM, Werner L, et al. Interlenticular opacification of piggyback intraocular lenses. *Int Ophthalmol Clin* 2001;41:47-62.
43. Gayton JL, Van der Karr M, Sanders V. Neodynium:YAG treatment of interlenticular opacification in a secondary piggyback case. *J Cataract Refract Surg* 2001;27:1511-1513.
44. Eleftheriadis H, Sciscio A, Ismail A, et al. Primary polypseudophakia for cataract surgery in hypermetropic eyes; refractive results and long term stability of the implants within the capsular bag. *Br J Ophthalmol* 2001;85:1198-1202.
45. Werner L, Apple DJ, Pandey SK, et al. Analysis of elements of interlenticular opacification. *Am J Ophthalmol* 2002;133:320-326.

46. Spencer TS, Mamalis N, Lane SS. Interlenticular opacification of piggyback acrylic intraocular lenses. *J Cataract Refract Surg* 2002;28:1287-1290.
47. Crone RA, Leuridan OMA. Unilateral aphakia and tolerance of aniseikonia. *Ophthalmologica* 1975;171:258-263.
48. Schechter RJ. Elimination of aniseikonia in monocular aphakia with a contact lens-spectacle combination. *Surv Ophthalmol* 1978;23:57-61.
49. Garcia M, Conzales C, Pascual I, et al. Magnification and visual acuity in highly myopic phakic eyes corrected with an anterior chamber intraocular lens versus by other methods. *J Cataract Refract Surg* 1996;22:1416-1422.
50. Rubin ML. Contemporary management of aniseikonia. *Surv Ophthalmol* 1997;41:321-330.
51. Beiley I, Lovie J. New design principles for visual acuity letter chart. *Am J Optom Physiol Opt* 1976;53:740-745.
52. Ferris Fl, Kassoff A, Bresnick GH, et al, New visual acuity chart for clinical research. *Am J Ophthalmol* 1982;94:92-96.
53. Werner L, Pandey SK, Izak AM, et al. Capsular bag opacification after experimental implantation of a new accommodating intraocular lens in rabbit eyes. *J Cataract Refract Surg* 2004;30:1114-1123.
54. Langenbucher A, Huber S, Nguyen NX, et al. Measurement of accommodation after implantation of an accommodating posterior chamber intraocular lens. *J Cataract Refract Surg* 2003;29:677-685.
55. Findl O. IOL movement by ciliary muscle contraction. In: Guthoff R, Ludwigh K, eds. *Current Aspects of Human Accommodation*. Heidelberg, Germany: Kaden Verlag; 2001:119-133.
56. Hays RD, Mangione CM, Ellwein L, et al. Psychometric properties of the National Eye Institute-Refractive Error Quality of Life instrument. *Ophthalmology* 2003;110:2292-2301.
57. McDonnell PJ, Mangione C, Lee P, et al. Responsiveness of the National Eye Institute-Refractive Error Quality of Life instrument to surgical correction of refractive error. *Ophthalmology* 2003;110:2302-2309.
58. McDonnell PJ, Lee P, Spritzer K, et al. Associations of presbyopia with vision-targeted health-related quality of life. *Arch Ophthalmol* 2003;121:1577-1581.

APPENDIX 1

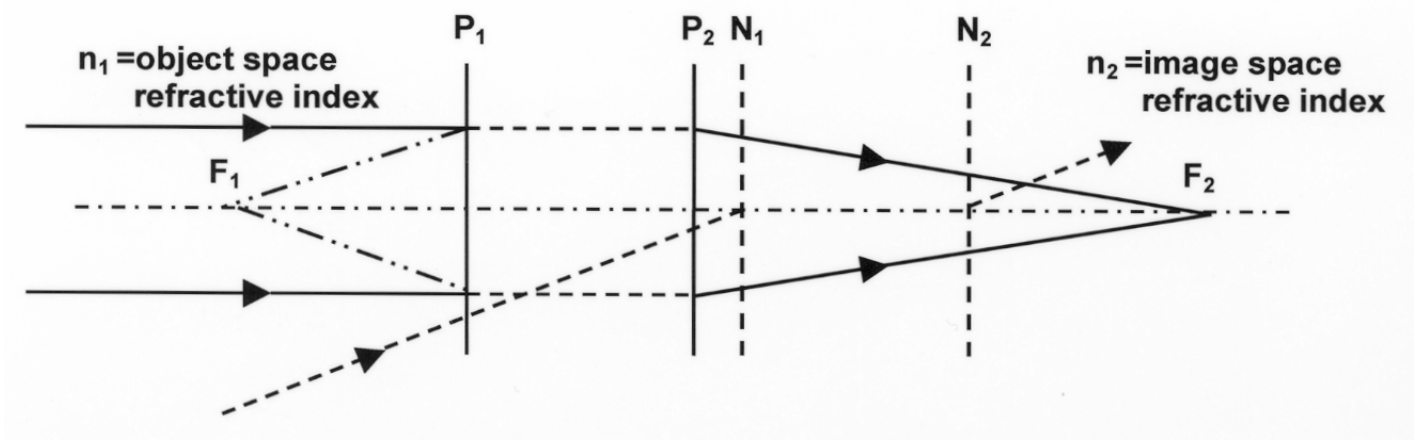

APPENDIX 1 FIGURE.

Power matrix modeling of magnification in a pseudophakic human eye: cardinal points (cardinal planes). The locations of the Principle planes (P_1 and P_2) and Nodal planes (N_1 and N_2) are different if the refractive indices in the object space and image space are different. The corresponding cardinal points are defined by the intersection of the system optical axis with the corresponding planes. The distance between the principle plane and corresponding focal point determines the effective focal length. The nodal planes are characterized by the property such that the angle at which a ray enters the nodal plane matches the angle at which it exits the other nodal plane. This implies that the image position is maintained as the system is rotated around the second nodal point. For instance, second nodal point in the eye system is close to the center of eye rotation, leading to insensitivity of the image location at the retina to small eye movements.

APPENDIX 2

PARAXIAL CHARACTERISTICS OF PSEUDOPHAKIC EYE WITH DUAL-OPTIC IOL

By convention, the locations of the cardinal points are defined in terms of the distances from the front surface (corneal vertex) in the object space and from the last surface (back surface vertex) in the image space. In case of the reduced eye model with the dual optic in place, the first surface is the composite corneal refracting surface and the last surface is the back surface of the dual-optic posterior lens. The locations used in the optical science definition are different from the locations used in anatomic descriptions, namely the front vertex of the cornea or the retinal plane. The optical science definition can be easily converted to the anatomical definition for known axial length L of the eye (Appendix 2. Tables A and B below).

APPENDIX 2. TABLE A. EYE MODEL PARAMETERS FOR THE DUAL-OPTIC INTRAOCULAR LENS (IOL)

MATRIX PARAMETERS	DEFINITION
First refraction surface = corneal surface K-reading	$R_1 = K = \frac{337.5}{r_1}$, where K = K-reading and r_1 = corneal radius*
First interspace = anterior chamber depth (ACD)	t_1 , n' = aqueous refractive index (1.336)
Second refraction surface = power of front surface or conventional IOL or front surface of anterior lens of dual-optic IOL	$R_2 = \frac{1000 \bullet (n_a - n')}{r_2}$, where n_a = refractive index of anterior lens material, n' = aqueous refractive index (1.336) and r_2 = surface radius
Second interspace = anterior lens thickness or conventional lens thickness	t_2 , n_a = refractive index of anterior lens material
Third refraction surface = power of back surface of conventional IOL or back surface of anterior lens of the dual-optic IOL	$R_3 = \frac{-1000 \bullet (n_a - n')}{r_3}$, where n_a = refractive index of anterior lens material, n' = aqueous refractive index (1.336) and r_2 = surface radius
Third interspace = separation between anterior and posterior lenses in the dual-optic IOL	t_3 , n' = aqueous refractive index (1.336)
Fourth refraction surface = power of front surface of posterior lens of the dual-optic IOL	$R_4 = \frac{1000 \bullet (n_p - n')}{r_4}$, where n_p = refractive index of posterior lens material, n' = aqueous refractive index (1.336) and r_4 = surface radius
Fourth interspace = posterior lens thickness	t_4 , n_p = refractive index of posterior lens material
Fifth refraction surface = power of back surface of posterior lens of the dual-optic IOL	$R_5 = \frac{-1000 \bullet (n_p - n')}{r_5}$, where n_p = refractive index of anterior lens material, n' = aqueous refractive index (1.336) and r_5 = surface radius

*Radii are in millimeters with conventional optical science sign nomenclature. The light travels from left to right, and the sign is positive if it is along the ray direction and negative otherwise.

APPENDIX 2 TABLE B. APPLICATION OF THE POWER MATRIX TO A MODEL EYE: DEFINITION OF CARDINAL POINTS AND THEIR DERIVATIVES

CARDINAL POINT OR ITS DERIVATIVE	FORMULA FROM THE POWER MATRIX DEFINED BY OPTICAL SCIENCE	ANATOMICAL OR EYE-RELATED DEFINITIONS
Lens T = Lens system total length	$T = \sum_{l=1}^{5} t_l$, distance between corneal and last refraction surface	Anterior Segment Length (ASL)
	$J = L - T$, where L = Eye Axial Length	Posterior Segment Length (PSL)

APPENDIX 2 TABLE B. (CONTINUED) APPLICATION OF THE POWER MATRIX TO A MODEL EYE: DEFINITION OF CARDINAL POINTS AND THEIR DERIVATIVES

CARDINAL POINT OR ITS DERIVATIVE	FORMULA FROM THE POWER MATRIX DEFINED BY OPTICAL SCIENCE	ANATOMICAL OR EYE-RELATED DEFINITIONS
First (Object) Focal Point	$F_1 = 1000 \bullet n \bullet \frac{a}{b}$ where n = object space refractive index = 1 (air)	Eye Focal Length
Second (Image) Focal Point	$F_2 = 1000 \bullet n' \bullet \frac{-d}{b}$ where n' = image space refractive index = 1.336 (aqueous)	
First (Object) Principal Point	$H_1 = 1000 \bullet n \bullet \frac{a-1}{b}$ where n = object space refractive index = 1 (air)	First (Object) Principal Point
Second (Image) Principal Point	$H_2 = 1000 \bullet n' \bullet \frac{1-a}{b}$ where n' = image space refractive index = 1.336 (aqueous)	Second (Image) Principal Point measured from cornea: $H'_2 = T - H_2$
First (Object) Nodal Point	$N_1 = 1000 \bullet \frac{a \bullet n - n'}{b}$ where n = object space refractive index = 1 (air) and n' = image space refractive index = 1.336 (aqueous)	First (Object) Nodal Point
Second (Image) Nodal Point	$N_2 = 1000 \bullet \frac{n - d \bullet n'}{b}$ where n = object space refractive index = 1 (air) and n' = image space refractive index = 1.336 (aqueous)	Second (Image) Nodal Point measured from cornea: $N'_2 = T - N_2$
First (Object) Focal Length = distance between First Principal Point and First Focal Point	$EFL_1 = 1000 \bullet n \bullet \frac{-1}{b}$	Eye Focal Length
Second (Image) Focal Length = distance between Second Principal Point and Second Focal Point	$EFL_2 = 1000 \bullet n' \bullet \frac{1}{b}$	
Image Distance = distance between Second Principal Point and Image Plan	$I = L - T + H_2 = L - H'_2$	
Image vergence in diopters	$V' = 1000 \bullet n' \bullet \frac{1}{I}$, where I = image distance	
Magnification = ratio of image size to object size	$M = 1 + \frac{b}{V'}$	Magnification
Object vergence in diopters	$V = -b - V'$	Object Vergence